Role of breathers in anomalous decay

E. Mihóková*
Institute of Physics, Academy of Sciences of the Czech Republic, Cukrovarnická 10, 162 53 Prague 6, Czech Republic

L. S. Schulman
Physics Department, Clarkson University, Potsdam, New York 13699-5820, USA

K. Polák
Institute of Physics, Academy of Sciences of the Czech Republic, Cukrovarnická 10, 162 53 Prague 6, Czech Republic

W. Williams
Physics Department, Clarkson University, Potsdam, New York 13699-5820, USA
(Received 7 January 2004; published 26 July 2004)

We have previously presented evidence for the formation of breathers in doped alkali halides subjected to a flash of UV light. Properties of these breathers, their phase space structure, robustness, decay, and propensity for formation, are studied here. Under a wide range of parameters and interionic potentials they form two-dimensional Kolmogorov-Arnold-Moser tori (less than generic) in phase space. Strobed views of these tori, useful in quantization, are shown. All features support the thesis of breather formation as the explanation for the luminescence decay anomaly that first motivated our breather proposal.

DOI: 10.1103/PhysRevE.70.016610 PACS number(s): 05.45.Yv, 78.55.−m, 31.70.Hq, 63.20.Ry

I. INTRODUCTION

Breathers are known to exist in a number of natural systems [1–3] (although nomenclature varies). In a series of studies of luminescence decay in doped alkali halides [4–11] it was found that the data could be explained by postulating extremely long relaxation times in the crystals. This factor-10^9 slowdown was in turn attributed to the formation of breathers in a lattice that is highly distorted by virtue of the Jahn-Teller effect [12]. In the present article we undertake a more general study of breathers in a nontranslationally invariant system, examining the effects of using different interatomic potentials, different atomic species (in particular different mass ratios for diatomic chains), and, finally, studying the effects of breather decay on the surrounding lattice. We confine attention to the zero-temperature case. An interesting result is that, at least for the parameter values we study, the phase space classical motion of the atoms lives on a two-dimensional Kolmogorov-Arnold-Moser (KAM) torus. That is, beyond the already particular property of regular, torus-confined motion, that torus only has two nonzero "radii," i.e., nonzero action variables. These studies were motivated by the results of Ref. [12], where the basic physical conclusions were established. The present work significantly firms up those conclusions, both physically and mathematically, by including material necessarily omitted in that brief article and by using techniques not employed there. The most illuminating of these is a stroboscopic method developed in Ref. [13] for viewing the KAM torus.

The study of nonlinear localized (in phase space) excitations has a long history, going back to Fermi, Pasta, and Ulam [14] and Kolmogorov (see Ref. [15]). In recent work (Refs. [16–28], as well as other sources to be cited in the sequel), much of it directed toward condensed matter applications, a variety of names has been employed for the excitations, including "soliton," and the more specific terms, "breather," "nonlinear localized excitations," and "intrinsic localized mode." We will use the term "breather."

Reference [12] was based on the analysis of a particular interionic interaction potential and drew its conclusions on the presence of breathers indirectly, for example from short-time approximate recurrences in the phonon excitation distribution. This followed the ideas in the classic Ref. [14]. While our recurrence was weaker than theirs in momentum space, we found substantial localization in coordinate space. We now have far more direct evidence of what is transpiring dynamically in the form of images of KAM tori and subsets of such tori, all of which confirm the original statements. Beyond this, the range of potentials for which breathers occur has been extended, so that the simple polynomial example of Ref. [12] is clearly *not* an exception; rather, breather formation is robust and generic. As indicated, even breathers that at first appeared to be quite messy, when analyzed stroboscopically turned out to live on two-dimensional KAM tori. This feature was present even when substantially more than the first two atoms on our chain (to be described below) were involved in the breather. Clearly this dimensionality is not related to the number of significantly participating atoms, and we now believe it to be a reflection of the *diatomic* nature of the solid. The stroboscopic analysis reveals loop subsets of the torus (easily understandable in an action-angle context). These loops play a vital role in the quantization of breathers [13], and the two-dimensionality augers well for the ability to calculate quantum levels in these systems.

Another thesis of Ref. [12] concerned the *relaxation* of

*Electronic address: mihokova@fzu.cz

the breather. However significant the slowdown of crystal relaxation, from picoseconds to milliseconds, it is nevertheless not a complete freezing of the lattice, so the gradual changes that do occur need to be explained within the breather context, a context that does not, in its pristine form, allow relaxation, except perhaps through Arnold diffusion. The lattice, however, is far from a pristine environment, and as discussed in Ref. [12] a breakdown in the Born-Oppenheimer adiabatic approximation can explain the ultimate relaxation. These matters will be studied in detail below.

A topic that did not come up in Ref. [12], but arises naturally from an overview of our observations, is the tantalizing issue of when one should expect anomalous decay. Some doped alkali halides show this effect, some do not. A full answer necessarily depends on subtleties of the Jahn-Teller effect as well as consideration of the sizes of lattice ions and impurities, but our breather work does add insight regarding one significant aspect: there appears to be a systematic dependence on the anion/cation mass ratio, and indeed this will be shown to be a consequence of the breather phenomenon.

In Sec. II we go into detail on the physical background. Section III describes how we go from the physical system to our model Hamiltonian. In Sec. IV the appearance of breathers in a variety of potentials is established and the dynamical structures associated with them explored. Issues of direct physical interest are covered in Secs. V and VI, the first devoted to a systematic discussion of implications of breather involvement on the appearance—or not—of a decay anomaly, the second to the connection between dissipative breather decay and the crystal relaxation pattern demanded by our decay-fitting articles [9–11]. In a final section we give an overview of our results.

II. PHYSICAL BACKGROUND

In Ref. [4] we reported anomalous decay in the slow-emission component of isolated centers in alkali halide crystals. For up to several milliseconds one sees much enhanced and nonexponential decay, going over finally to an exponential. This pattern was observed for Tl^+ and Pb^{2+} centers in various alkali halide hosts, with both fcc [5–7] and bcc [8] structure. The pressing question became: Is this intrinsic or is it a consequence of crystal defects or other irregularities of the luminescent center environment? Nonintrinsic explanations were systematically excluded through improved crystal preparation, sample annealing, impurity dilution, and other cautionary measures described in Ref. [9] (in particular cases other explanations may apply [29], but not for the full range of observed phenomena).

Optical properties of isolated Tl or Pb centers in alkali halide crystals can be described by considering the impurity and its six nearest neighbors (in the fcc lattice) to be a quasimolecule [30,31]. When excited, the molecule distorts according to the Jahn-Teller (JT) effect and its lowest excited state consists of two levels—a *radiative* level, displaying exponential nanosecond decay, and a *metastable* level, with a millisecond time scale. The latter is the level for which the anomaly is observed. To explain the anomaly we proposed that the lattice took a long time to yield to the strain, thereby introducing a coupling between the idealized $PbBr_6$ levels. Systems in the metastable level then transited to the radiative level from which they rapidly decayed. This assumption allowed successful fitting of liquid He temperature KBr:Pb data [9], provided that the ultimate relaxation of the lattice is on the same time scale as that of the slow emission decay (ms). The model was extended to the entire collection of Pb- and Tl-doped alkali halides both at liquid He temperature [10] and at higher temperatures [11], enabling us to give an accounting of the entire range of phenomena, including the gradual extinction of the anomaly as the crystal warms.

Having related the decay anomaly to slow-lattice relaxation, the next issue was the origin of the slowdown. One candidate was tunneling, a phenomenon that often spans a wide range of scales (i.e., for which large or small dimensionless numbers can occur). Such barrier penetration could be involved in the following way. Due to the JT deformation the nearest neighbors of the Pb (or Tl) ion after excitation are forced to significantly change their previous equilibrium positions. A rigid lattice could resist this push until random thermal motions allowed a breakthrough. This sudden-change hypothesis could be tested, because the temporal pattern of decays is different from that associated with continuous lattice deformation. It was found [11] that the data fits were less satisfactory than those obtained from the exponential or power law relaxation function used [9–11] in most of our work.

We came to the explanation that we now consider most likely through modeling the dynamics of the lattice [12]. We found that under classical dynamics the energy of the extended quasimolecule was confined to a small neighborhood of the Pb-excitation-induced perturbation, a perturbation significant enough to make nonlinear effects important. This confinement in turn led to a slowdown in relaxation, in particular with the pattern needed to account for the experimental data.

III. MODEL

We focus on a particular substance, $KBr:Pb^{2+}$. For this crystal and this impurity the excitation-decay scenario begins with a flash of UV light that excites the Pb and leads to a JT symmetry-breaking distortion. The $PbBr_6$ quasimolecule goes from octahedral symmetry to a lower tetragonal symmetry, stretching [32] along one of its axes. We assume that the Br immediately next to the Pb and along the axis of deformation is under tremendous pressure to move away from the Pb. We further assume that in studying the effect of this force we can confine attention to the line of atoms on this axis, effectively a chain, with the influence of the rest of the crystal expressed through a "holding force." We introduce this substrate-defining force through a potential felt by each ion on the chain; it defines the equilibrium position of the ion in the crystal in the *absence* of the specific pressure from the displaced Br. Note that the nonisotropic stresses imply lesser deformation for off-axis atoms.

It should be clear that we do not look upon this as an *ab initio* calculation of the mechanism of slow crystal relax-

ation, or even as a prediction that such relaxation *must* occur. Rather we begin from the experimentally observed decay anomalies and their systematic explanation for a range of crystals, impurities, and temperatures, using the hypothesis of slow crystal relaxation. Such relaxation, *slowed by a factor of a billion*, demands explanation. The breather occurring in our model system provides such an explanation.

We assume an interionic potential $V(u)$ with u the displacement from the ion's equilibrium position. For the simulations reported in Ref. [12] we used $V(u)=M\omega_0^2(u^2+\lambda u^4)/2$. A quadratic potential would not be adequate because the JT distortion is known to induce a displacement of up to 15 or 20% of the ionic spacing [33]. The Hamiltonian is

$$H=\sum_{n=1}^{N}\left\{\frac{P_n^2}{2M}+\frac{rp_n^2}{2M}+V(q_n-Q_n)+V(Q_n-q_{n-1})+\nu[V(Q_n)+V(q_n)]\right\}. \tag{1}$$

Q_1 is the Br ion to the right of the Pb, followed by q_1 (a K ion), Q_2, etc. The Q particles have mass M, the q's, M/r. The "holding force" arises from the potentials multiplying ν, so that ν can be interpreted as an effective number of neighbors. In some simulations (but not in this article) we used $\tilde{V}(u)\equiv V(\sqrt{u^2+a^2}-a)$ for this holding force, with a the lattice constant. For KBr, $r\approx 2$. This Hamiltonian, describing only Br and K, includes the effect of the highly distorted Pb wave function through the nondynamic variable q_0. By setting this to specific positive values we can provide a push on the entire chain, inducing intense oscillation, possible breather formation, and possible wave propagation, depending on the model parameters.

In Ref. [12] the system was solved numerically for the indicated potential, using units such that $M=1$ and $\omega_0=1$. In the present article we study a more general class of potentials, introduced below. The significant phenomenon described in Ref. [12] is that with $\lambda=1$, $r=2$, and $\nu=4$ the energy deposited by the nonzero q_0 [in practice, q_0 was O(1)] remained substantially confined to a small neighborhood consisting of the first two ions. This property will concern us for the other potentials as well.

Throughout this article we assume that the system is at zero temperature. This means that except for the stresses induced by the JT distortion the atoms are initially at rest. In practice we have found that introducing a bit of noise (corresponding, say, to the actual experimental value of 4 K) into the system does *not* destroy the breather—in fact it hardly disturbs it. A related issue is our taking q_0 to be a nondynamic quantity. Essentially this means ignoring the motion of the expanded Pb atom, and is justified by the symmetry of the Jahn-Teller distortion (expansion or contraction). In effect our work is a study of symmetric excitations of a chain extending in both directions. Other excitations, induced perhaps thermally, could be considered for the finite-temperature case.

Interatomic potentials

There are a number of potentials that are popularly used for the description of interatomic forces. We mostly use the notation of Ref. [23], an article that also addresses nonlinearity-induced localization [34].

Polynomial interatomic potential:

$$V_P(x)=M\omega_0^2\left[\frac{1}{2}x^2+\frac{\kappa}{3}x^3+\frac{\lambda}{2}x^4\right]; \tag{2}$$

M and ω_0 are taken to be 1 in our work.

Morse interatomic potential:

$$V_M(x)=P(e^{-ax}-1)^2. \tag{3}$$

Born-Mayer-Coulomb interatomic potential:

$$V_{BMC}(x)=\frac{\alpha_M q^2}{d^2}\left[-\frac{d^2}{x+d}+\rho e^{-x/\rho}+d-\rho\right]; \tag{4}$$

α_M is the Madelung constant, q is the effective charge, d is the distance between adjacent particles, and ρ describes the repulsion between atoms.

The Toda potential $[V(x)=(a/b)e^{-bx}+ax-a/b]$ and Lennard-Jones potential $(V(x)=\epsilon\{[d/(x+d)]^{12}-2[d/(x+d)]^6+1\})$ are also often used, but we did not examine their breather-formation properties.

IV. THE BREATHER IN A VARIETY OF POTENTIALS

In this section we report lattice dynamics simulations using the potentials of Eqs. (2)–(4). Figure 1(a) presents the results of a simulation using our original polynomial interatomic potential, Eq. (2). The kinetic energy as a function of time and atomic number provides a nice illustration of what we call *confinement*. Together with the time dependence of the atomic position coordinate (in the inset) it shows that the energy is substantially confined within the first two atoms of the chain. The energy deposited in the chain by the JT deformation does not propagate but becomes bound in vibrations of the first atoms of the chain, i.e., the breather. This lack of energy propagation lies behind the significant slowdown in crystal relaxation and is the origin of the decay anomaly, as discussed in Ref. [12] and elaborated below.

The frequency spectrum of the first four atoms, obtained by fast Fourier transform (FFT) of $Q_1(t)$, $q_1(t)$, $Q_2(t)$, $q_2(t)$, is displayed in Fig. 1(b). Because we use finite-interval FFT, a sharp line in the true spectrum becomes widely spread, and finding maxima in the FFT spectrum is not sufficient to extract true single frequencies. Takatsuka [35] has studied this problem and for a single pure frequency the extraction procedure is straightforward (see Ref. [13] for the precise implementation of the method in our case). Later in studying the Born-Mayer-Coulomb (BMC) potential we will discuss improvements. In any case, in Fig. 1(b), the spectrum shows two dominant frequencies falling above and below the optical phonon band. These frequencies characterize the oscillations of the breather. The position of the phonon bands relative to the rest of the spectrum is marked by a sequence of horizontal lines. It is important, with respect to the localiza-

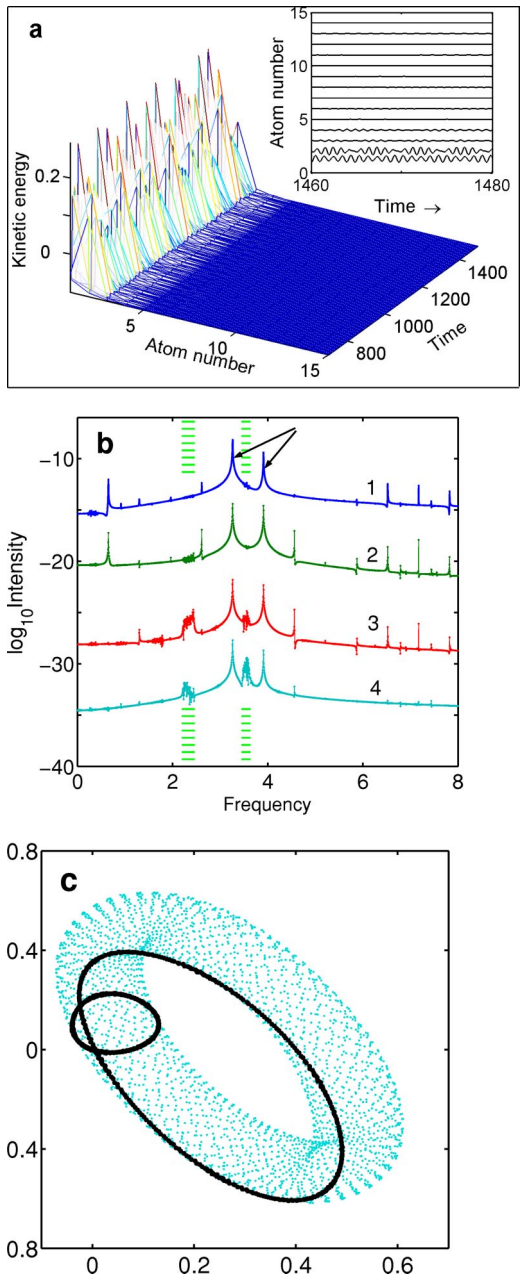

FIG. 1. Quartic polynomial interatomic potential. (a) Kinetic energy of the system as a function of time and atom number. The inset shows the positions of the atoms vs time. (b) Fourier transforms (intensity) of the functions $[Q_1(t), q_1(t), Q_2(t), q_2(t)]$ in curves 1 – 4. The curves corresponding to successive atoms are vertically shifted (downward by 4) for better display. The superimposed horizontal lines indicate where the phonon frequency bands are. Arrows point to the principal frequencies of the spectrum outside the phonon bands. All other intense frequencies are resonances or beat frequencies of these two. (c) The KAM torus, projected on a plane within the four-dimensional space $\{Q_1, P_1, q_1, p_1\}$. Each figure contains 100 000 points, with 100 points taken per system time unit. The abscissa is position and the ordinate momentum in the units described in the Appendix. Loops in the torus represent projections on the Q_1-P_1 and q_1-p_1 planes of the stroboscopically viewed KAM torus, substantiating the assertion that the torus is two dimensional (only has two significant nonzero radii). The parameters used in the simulation are $N=20$, $q_0=1$, $r=2$, $\nu=4$, and $\lambda=1$.

tion of the excitation, that the breather frequencies do indeed fall outside the phonon bands. Note too that because our model imposes a holding force to simulate atoms not included in the model, important phonon modes are missing. In particular, low frequency modes, allowed in a true crystal, do not occur in the model. As a consequence, the acoustic phonon band does not start from zero frequency.

In Fig. 1(c) we show a projection of the KAM torus which is the classical phase space orbit of the breather. Superimposed is a pair of loops, which result from a stroboscopic image of the torus. As developed in Ref. [13], the ability to produce such a figure takes advantage of the existence of a transformation (à la KAM), albeit a singular and unknown one, to action-angle variables such that the Hamiltonian is a function of the action variables only. With $\{J_1, \theta_1, \ldots\}$ the variables, the torus is given by the equations $\theta_k = \omega_k t + \theta_{k0}$ (with $\omega_k = \partial H / \partial J_k$), $k = 1, \ldots, N$ and N the number of coordinate degrees of freedom of the system. If one knows one of the ω_k's, then by viewing the full orbit only at multiples of $2\pi/\omega_k$ a torus of one lower dimension is generated. These are the loops of Fig. 1(c), one for each of the dominant frequencies. The fact that these are clean, one-dimensional loops implies that the KAM torus for our simulations is only a two-dimensional structure [36]. This is of course consistent with the presence of only two dominant frequencies outside the phonon bands in the frequency spectrum although there is no *requirement* that only two frequencies appear. The original momenta and positions are nonlinear functions of the action-angle variables, so that in analyzing Q_1 and other functions, one can certainly obtain beats and multiples of the "true" ω's (even with only two nonzero action variables).

The addition of a relatively strong cubic term to the polynomial interatomic potential Eq. (2) again provides strong kinetic energy confinement [Fig. 2(a)]. The frequency spectrum [Fig. 2(b)] appears to be somewhat richer but a frequency analysis show that again only two dominant frequencies are present and all other intense frequencies are merely resonances or beat frequencies of these two. The result is confirmed by a view of the corresponding KAM torus with two clean loops when viewed stroboscopically [Fig. 2(c)].

For simulations of chain dynamics with Morse and Born-Mayer-Coulomb (BMC) interatomic potentials, Eqs. (3) and (4), the parameters entering potentials were chosen in such a way that the potentials are somewhat "softer" than the polynomial potential. Nevertheless, as Figs. 3(a) and 4(a) show, they too provide substantial kinetic energy confinement extended to the region of the first five to six atoms of the chain. Frequency spectra in Figs. 3(b) and 4(b) appear to have several dominant frequencies, but there still turn out to be only two truly independent frequencies, corresponding to two degrees of freedom of the system represented by two-dimensional KAM tori in multidimensional phase space [Figs. 3(c), 4(c), and 4(d)].

The two-dimensional Morse and BMC tori eliminate one argument that might have seemed reasonable to justify the low KAM torus dimension in the other cases. For the quartic polynomial potential, for most of the parameter values we analyzed in detail, hardly more than two atoms were substantially involved. Atoms number 3 and 4 do have a small percentage of the energy, but you might have argued that with

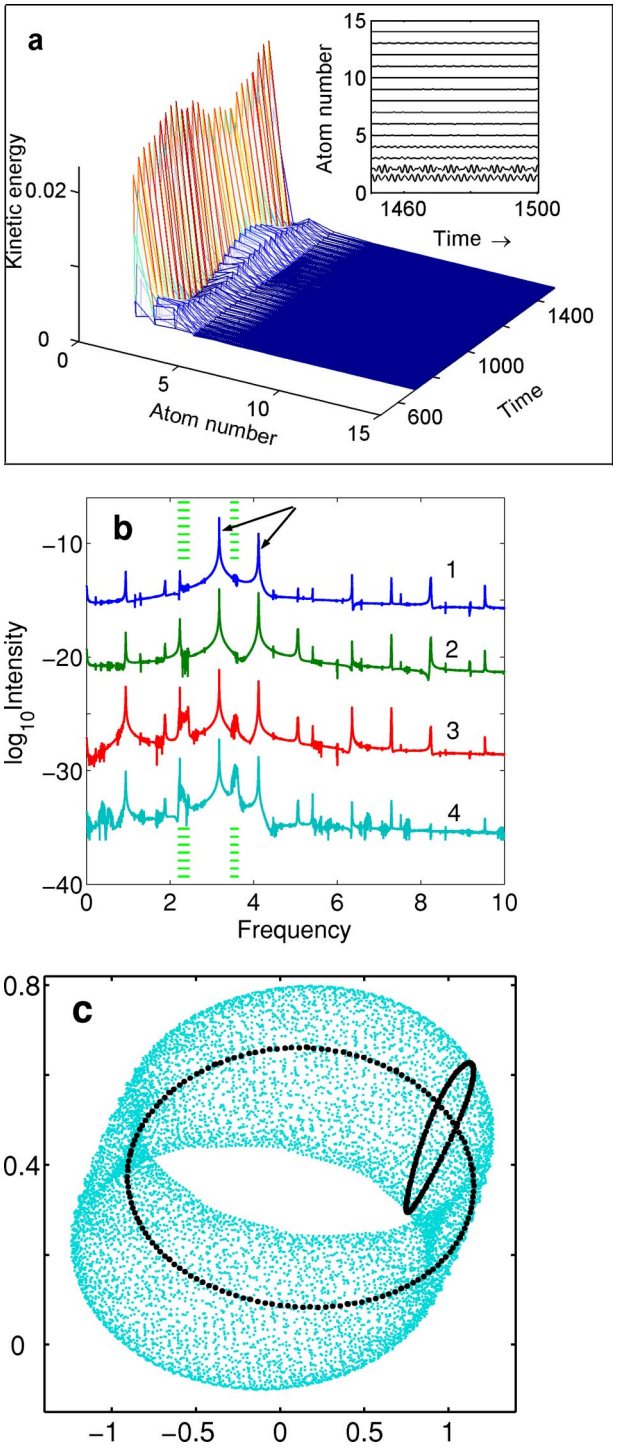

FIG. 2. Polynomial interatomic potential, including a cubic term. (a), (b), and (c) as in Fig. 1. Parameters used in the simulation: $N=20$, $q_0=1$, $r=2$, $\nu=4$, $\lambda=1$, and $\kappa=-1$.

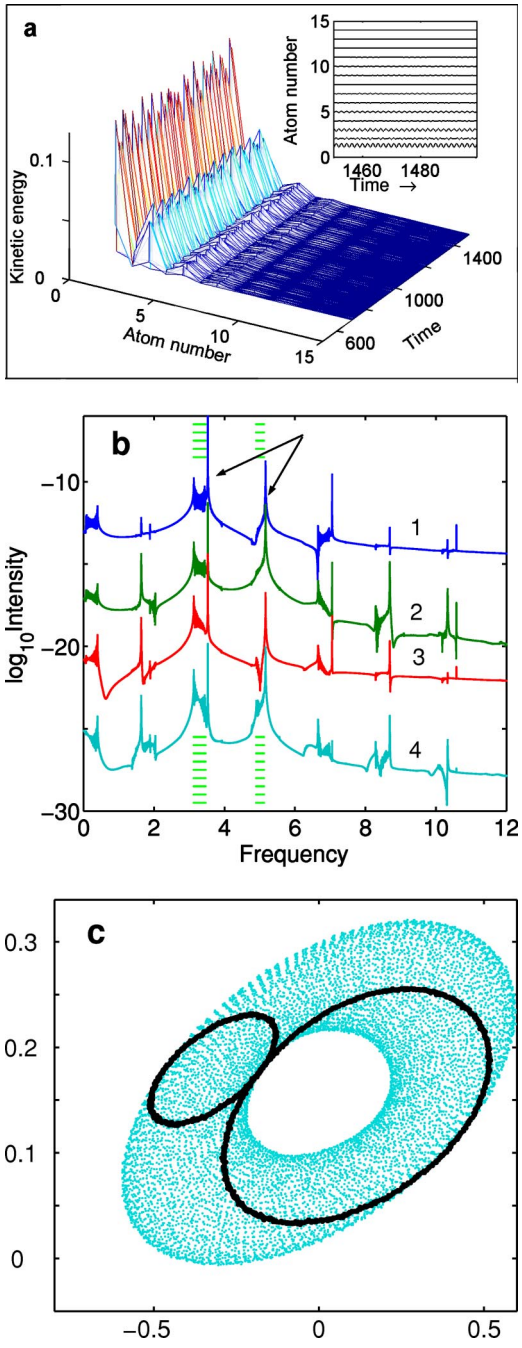

FIG. 3. Morse interatomic potential. (a), (b), and (c) as in Fig. 1. Parameters used in the simulation: $N=20$, $q_0=1$, $r=2$, $\nu=4$, $P=4$, and $\alpha=0.5$.

most of the energy localized on only two coordinates the KAM torus would be similarly confined in phase space. But for BMC and Morse, four or five atoms move appreciably.

Determination of the dominant frequencies of the breather with high accuracy (five digits) is the most important issue for establishing the number of degrees of freedom of the breather, or the dimension of the KAM torus. For the BMC potential we needed to apply a special "cleaning mechanism" to the frequency spectrum. Two problems were at work. First there is a finite size effect: although most energy (due to nonzero q_0) remains in the breather, a small amount is typically radiated away. When this bounces off the far boundary (at the 40th atom in our simulations) it will return to disturb the breather. This reflection (which is artificial anyway) damages the breather in no significant way (the breather is robust, as observed earlier in connection with noise), but the perturbation does disturb the delicate estimates of frequency that are necessary for stroboscopic analysis.

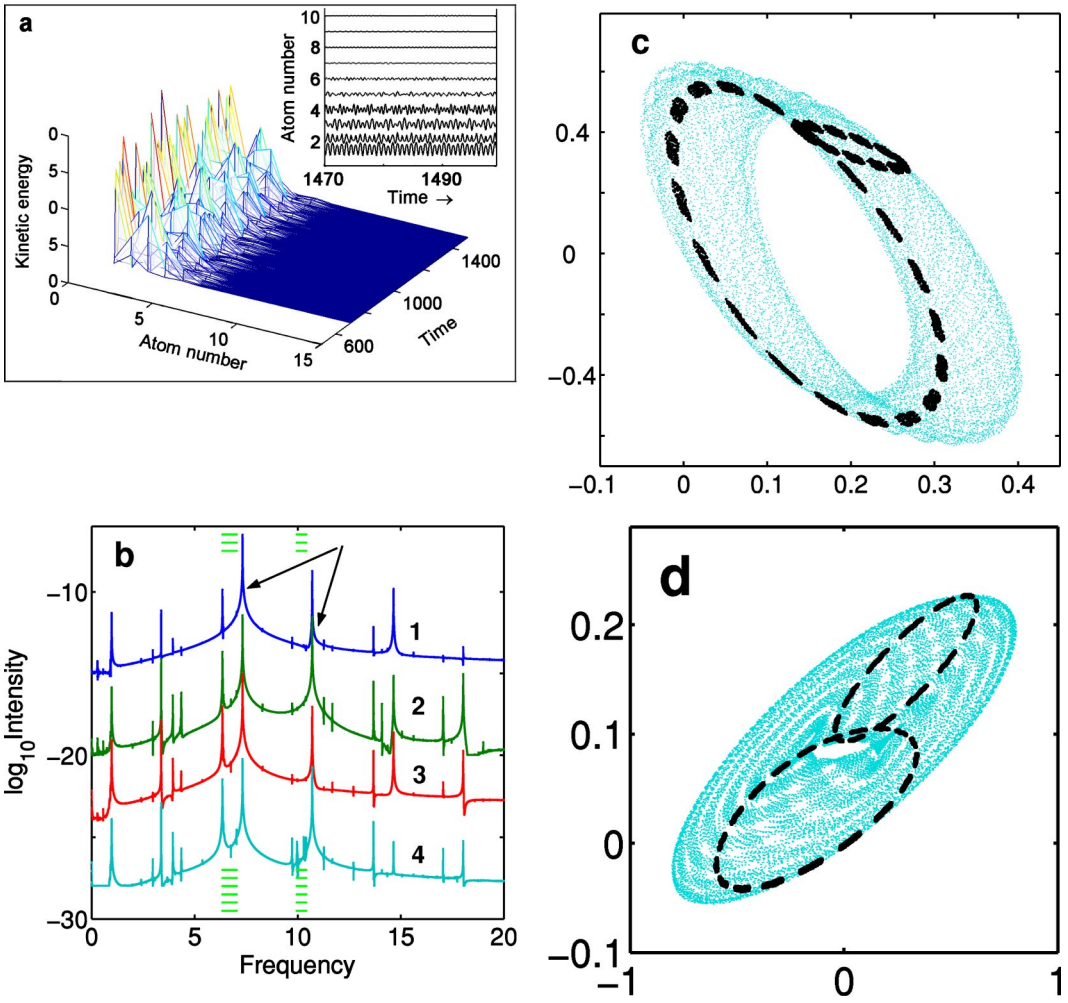

FIG. 4. Born-Mayer-Coulomb potential. (a), (b), and (c) as in Fig. 1. (d) The KAM torus projected on a different plane. Parameters used in the simulation: $N=20$, $q_0=1$, $r=2$, $\nu=4$, $\alpha_M q^2/d=10$, $\rho=0.3$, and $d=3.3$.

Second, and more fundamental, is that quite a few additional frequencies show up in the BMC spectrum. As it later turned out this was *not* because the dimension of the torus was greater than 2, but (we believe) is the result of the transformation from action-angle variables being more nonlinear than for the other cases. The first problem was dealt with by putting a damping force on the last atoms of the chain so that the energy that reached the boundary was dissipated and did not reflect. This does clean up the spectrum a bit. As indicated, our determination of frequency used a method of Takatsuka [35] (as implemented in Ref. [13]). In fact Ref. [35] is particularly devoted to determining frequencies when two frequencies are close to one another. The BMC spectrum was more complicated yet, with a background of what appear to be many frequencies. We dealt with this by using the single frequency method of Ref. [35] and then using properties of classical mechanics to improve upon it. A stroboscopic view with the raw initially derived frequency gives a rather fragmented image, but by searching nearby frequency values lovely loops emerged, and in fact only *two* of them (for the two principal raw frequencies). In Ref. [13] the sharpness of the strobed loops served as a check on frequency; now it becomes a yet finer tool for ascertaining the true underlying classical values.

Study of the chain dynamics with the foregoing collection of interatomic potentials confirms that the confinement phenomenon, which in our situation means breather formation, is not a property of a specific choice of interatomic potential. Rather it is a characteristic feature of the dynamics.

V. PREDICTIONS OF THE MODEL WITH RESPECT TO ANOMALIES IN A RANGE OF SUBSTANCES

The decay anomaly has been observed in a variety of doped alkali halides. Our experimental work reported in Ref. [10] shows systematic behavior of the anomaly when the host lattice is changed. Namely, for potassium halides doped either with Tl^+ or Pb^{2+} the anomaly grows (the nonexponential part of the decay is steeper and/or survives to longer times) with increasing size and mass of the lattice anion. This occurs in the sequence of lattices KCl→KBr→KI. For the KCl lattice the anomaly is small (Tl^+) or nonexistent (Pb^{2+}); for KBr it is big, for the KI lattice very big. The objective of our decay model was the phenomenological description of these data based on the assumption of slow lattice relaxation, an assumption whose detailed implementation is expressed through a number of parameters that

entered the theory. Experimental data in Ref. [10] were successfully fit and the parameters of the model showed systematic trends. Our preliminary experimental results with Pb^{2+}-doped NaBr and RbBr crystals show that similar behavior is observed in the sequence of lattices RbBr→KBr →NaBr where the lattice cation is successively made smaller and lighter. Namely, for the RbBr crystal a weak anomaly is observed while there is a significant anomaly for Pb-doped KBr and NaBr crystals. To summarize, a quantity that certainly affects the character of the decay anomaly is, r, the ratio of the mass of the lattice anion to that of the lattice cation. In the sequence of potassium halides (KCl→KBr →KI) the corresponding mass ratio changes as $r\sim 1$ to $r \sim 2$ to $r\sim 3.3$. In the sequence of alkali bromides (RbBr →KBr→NaBr) the mass ratio goes from $r\sim 1$ to $r\sim 2$ to $r\sim 4$. Systematically comparing the anion-cation mass ratio with the character of the decay anomaly one sees that from the experimental point of view a very slight anomaly is observed—or none at all—for mass ratios close to 1, while for ratios of 2 or more the anomaly is large. How is this observation consistent with our breather model?

To study this we used our standard polynomial potential, that which produced our original breather. We performed lattice-dynamics simulations changing the atomic mass ratio entering the chain model. It turns that different mass ratios can be more or less favorable for forming the breather. The simulations were made for a chain of 40 atoms. As a measure of how "good" the breather is, which is to say, how good is the confinement of the energy to the region of the impurity, we calculated a kinetic energy-weighted position. That is, let k be the atom number, $k=1$ for the immediate neighbor of the impurity, and counting outward. Let $w_{KE}(k)$ be the average kinetic energy of the kth atom. Then

$$k_{KE} \equiv \langle k \rangle = \frac{\sum_k k\, w_{KE}(k)}{\sum_k w_{KE}(k)}. \tag{5}$$

The smaller this quantity is, the more the energy is concentrated in the breather, and therefore the bigger the expected decay anomaly. We chose this measure of confinement because of the usefulness of the kinetic energy plot [see part (a) of Figs. 1–4] for immediate recognition of the confinement phenomenon. The result of a systematic study of k_{KE} as a function of r is shown in Fig. 5. Note that for the parameters used, as $r\to 1$, there is a kind of phase transition, namely $k_{KE}\to\infty$, where "∞" for this finite lattice means halfway to the boundary, i.e., a delocalized excitation. We have not determined whether there is any sharp transition in a phase transition sense; this also seems irrelevant for the physical system at hand, because of the ultimate need to quantize.

In any case, a mass ratio higher than 2 is favorable for forming a breather and most of the kinetic energy is trapped in first atoms of the chain. For mass ratios near one most of kinetic energy travels away. This is completely and satisfyingly consistentwith the experimental observations.

Additional support for the breather mechanism comes from studies of the *same* substance, undergoing JT deformation along *different* axes. This will be reported in detail elsewhere, but we mention at this point that when the JT axis does not provide a chain of nearest neighbors, there is essentially no anomaly. It is known that the quasimolecule associated with an isolated impurity and its nearest neighbors in alkali halide crystals under excitation undergoes JT distortion either along tetragonal or trigonal axes. Some substances show two emission bands: one is called the A_T emission and is related to a tetragonal distortion, the other, A_X emission, is related to a trigonal distortion. With respect to potential breather formation these distortions are quite different. In one case (A_T, tetragonal) there is a line of nearest-neighbor atoms, allowing the physical picture described throughout this article. In the other (A_X, trigonal) direction there is no chain of nearest neighbor atoms. Experimentally we have observed both emissions for KBr:Tl and NaBr:Pb crystals. In both crystals the anomaly was observed only for the slow component of the A_T emission, while A_X emission decay showed no anomaly. Decay anomalies previously reported by us (including a large variety of substances) have *always* been associated with the A_T band [37].

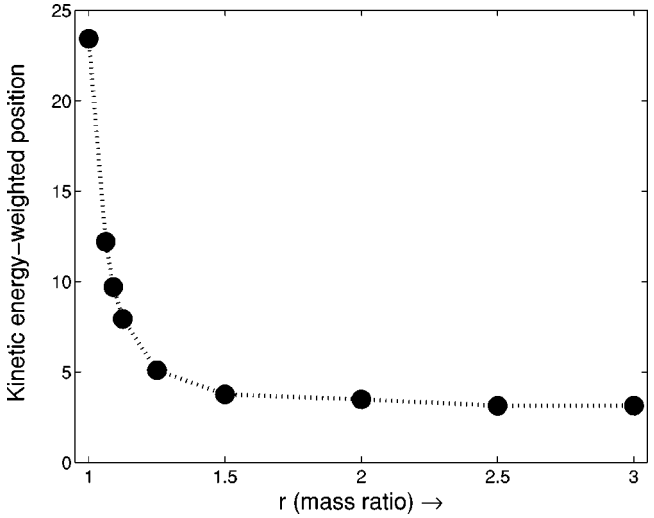

FIG. 5. Kinetic energy-weighted position (in atomic spacing units) as a function of anion-cation mass ratio. For details see the text. The parameters used in the simulation are $N=20$, $q_0=0.5$, $\nu=4$, and $\lambda=0.25$.

VI. BREATHER DECAY AND LATTICE RELAXATION

Breathers are a two-edged sword: they can indeed inhibit lattice relaxation, but on the face of it, it would seem they should *stop* the process, not slow it. This is because once formed, they should last forever. In principle, they can morph into other excitations by the process of Arnold diffusion (although it has been suggested [38] that the number of *effective* degrees of freedom here precludes Arnold diffusion). However, the time scale for that process is a delicate function of the dynamical parameters and should be subject to significant variation from substance to substance. Instead we find crystal relaxation (and presumably breather decay) always to be on the same time scale as that of the metastable level, too much of a coincidence.

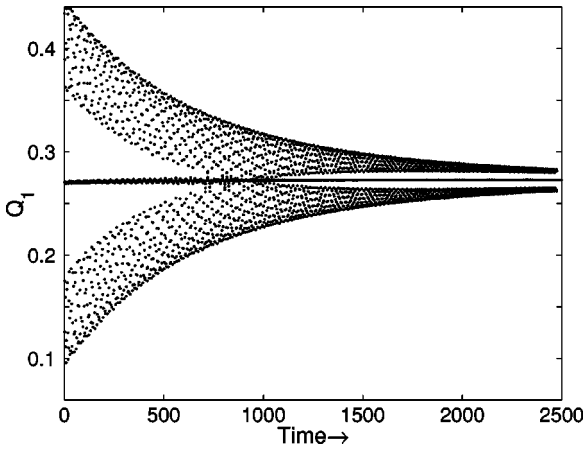

FIG. 6. Relaxation of Q_1. Points represent maxima and minima of Q_1's oscillations. The curve in the middle is obtained by averaging.

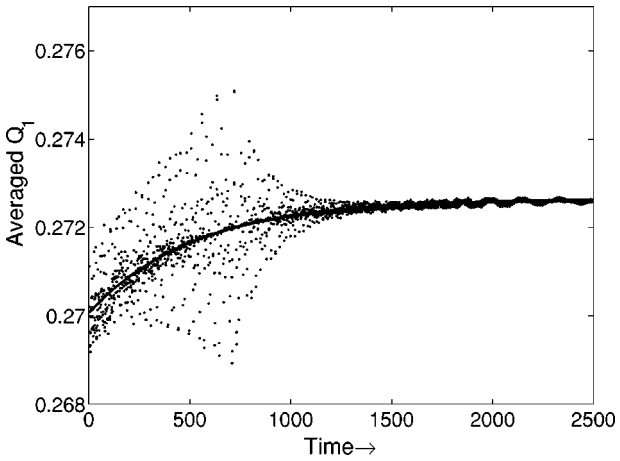

FIG. 7. Relaxation of the average of Q_1. Points represent averaged values of Q_1 (detail of the curve in Fig. 6). The solid curve is a fit to the data by the function $r_0+\Delta r[1-\exp(-\Gamma t)]$. Parameters used in the simulation are as in Fig. 1; the damping imposed on the first atom is $\gamma=0.005$, and the lattice relaxation resulting from the fit is $\Gamma=0.0019$.

For this reason we considered whether the mechanism of metastable-level decay could operate as well on the breather. Now the decay of the A_{1u} metastable level [39] to the A_{1g} ground state in say, KBr:Pb, is electromagnetically forbidden. This leaves vibronic interactions as a decay mechanism, and it is believed that decay occurs via a mode possessing T_{1g} symmetry [40,41]. In practice this means that ions in the neighborhood of the quasimolecule interact with, and carry energy away from, the quasimolecule wave function. We postulate that the Br at the head of our chain, which is in fact part of the quasimolecule, interacts dissipatively (violating the assumptions of the Born-Oppenheimer approximation) with the electronic wave function, allowing energy to pass via this nonclassical route to other—nonchain—degrees of freedom. As remarked in Ref. [12] the similarity of the matrix elements for the two processes brings them to the same time scale. The way we modeled this additional interaction classically was to add a dissipative force acting on the dynamical variable Q_1. We took this to have the simple form $-\gamma\dot{Q}_1$.

Physically, the value of γ should be on the order of 10^{-9}, taking one from the natural picosecond scale of ionic vibrations (in our units $\omega_{\text{Debye}}\sim\omega_0=1$) to that of metastable decay, milliseconds. By the way, this also implies that the Born-Oppenheimer approximation, which underlies our use of effective interatomic potentials, is perfectly valid on its intended scale $[O(10^{-3})]$. With the dissipative term the motion of Q_1 continues its usual oscillations, with a slow, systematic movement of its center of motion. It is this movement that represents the crystal relaxation. For this reason, to see the effect of γ we had to average the motion. This was done by finding the values of successive maxima and minima of Q_1 and averaging in pairs. Small oscillatory motion (still on the ps scale) remained and three or four more successive-pair averages were performed. In Fig. 6 we show the positions of the oscillation extremes as well as the result of a few averages. Since the scale of oscillation greatly exceeds the gradual movement of Q_1's center, a separate plot of the central line in Fig. 6 is shown in Fig. 7. Superimposed on the points is a fit by a function of the form $r_0+\Delta r[1-\exp(-\Gamma t)]$, with parameters r_0, Δr and Γ. This is precisely the form we used in Ref. [9] and subsequent articles for the gradual relaxation of the effective crystal coordinates. The value of $r_0+\Delta r$ was not varied (i.e., it was not a free parameter, and was taken equal to the equilibrium value of Q_1 in the presence of nonzero q_0), but Γ and r_0 were adjusted to minimize mean square error. In the simulation γ was taken of order 10^{-3}, since running the simulation for 10^9 time units was out of the question, and in any case was irrelevant for establishing the matter of principle. The value of Γ resulting from the fit was typically (for a variety of other run parameters) about 30–40% of γ, in line with simple dynamical models of dissipation.

VII. DISCUSSION

For doped alkali halides, the existence of breather modes provides an answer to a long-standing puzzle that arose in the decay of luminescence, where such crystals were illuminated with a UV flash and the "slow" component emission took place much more rapidly than expected, moreover, with a decidedly nonexponential temporal pattern. We first made the case for this in Ref. [12], and in the present article have marshalled additional evidence in support. In Ref. [12] we found that breathers formed when the interatomic potential was a quartic. In the present paper breather formation occurs when the potential has cubic terms, when the potential has the Morse form [Eq. (3)] and when it has the Born-Mayer-Coulomb form [Eq. (4)]. From this we conclude that breather formation is a robust feature. A different perspective on this robustness arises when random noise intrudes. Although we have here focused on zero-temperature phenomena, we mention that the introduction of noisy initial conditions at about the level of 4 K (at which temperature the experiments of Refs. 9 and 10 took place) hardly affects the essential breather features.

We have systematically studied the breathers associated with the various nonlinear, but nevertheless quite different, potentials, and have found that their similarities went beyond the fact of confinement (by which we mean that the vast majority of the energy of the external blow does not radiate away). A compelling demonstration of breather formation is the mapping of the KAM torus, which is the orbit in phase space of the classical motion. We used a stroboscopic method of viewing this torus (developed for quantization purposes [13]) which allowed the further observation that there were only two nonzero radii (or action variables) for the torus. The clean loops, by the way, also demonstrate that the torus is hollow. From the two-dimensional projections alone this is not evident, and a gradual extinction of the excitation could be taking place, but apparently this is not the case.

This observation has further implications for the semiclassical quantization process; in particular, it means an easier task. The main difficulty in that quantization (as implemented in Ref. [13]) is the evaluation of action integrals, whose (numerical) difficulty would increase with an additional torus dimension.

A propos the two-frequency observation, there is interesting work by Flach, Willis, and Olbrich [42] in which instabilities in localized excitations are observed when more than one frequency is present (basically because of the overlap of sums of frequency multiples with phonon frequencies). On the time scale of our (numerical) observations this effect is not seen, but our integrations do not extend as far as theirs. With respect to our fundamental physical phenomenon, even if one breather mode disappeared we would still expect slow crystal relaxation. This is because for what seem the physical conditions for our experiments, the actual breather is dominated (on a scale of about 5 to 1) by a single one of the breather modes [13], and it alone could provide the relaxation inhibition.

Other physically significant aspects of the breather were checked. Systematic physical observations suggest that alkali halides for which the anion-cation mass ratio is close to 1 have little or no anomaly in their luminescence decay. We find here that breather formation exhibits a similar effect: as this ratio approaches unity the breather gets more and more delocalized, and for appropriate parameters disappears completely.

An important adjunct to our breather work is its specific effect on lattice relaxation. A study of this effect was offered here (improving on the demonstration in Ref. [12]) and shows how breather relaxation can provide precisely the pattern of lattice movement used in our data fitting schemes [9–11].

ACKNOWLEDGMENTS

We thank S. Flach, J. Fleischer, V. Fleurov, B. Gaveau, and M. Nikl for useful discussions and suggestions. This work was supported by NSF Grant Nos. PHY 97 21459 and PHY 00 99471 and by Czech Grants No. ME587 and ASCR No. A1010210.

APPENDIX: UNITS AND PARAMETERS

The units used in our simulations are as follows.

(a) Angstroms for distance.

(b) The mass of Br is unity and the ratio "r" is 2, which is the approximate Br to K mass ratio. The factor "M" in $V(u)$ [see its definition, following Eq. (1)] is thus unity.

(c) The Debye temperature of KBr is taken to be 173 K.

(d) The time unit is $1/\omega_0$, with ω_0 the frequency in $V(u)$. Thus ω_0 also becomes unity. The relation between ω_0 and ω_{Debye} was discussed in Ref. [13] and in the present notation is given by $\omega_0=\omega_{\mathrm{Debye}}\sqrt{2(1+1/r)}/[(6\pi^2)^{1/3}]$.

In these units $\hbar$ is approximately 0.007 897, one unit of energy is about 0.839 eV and the time unit close to 0.1 ps. Note that these values are sensitive to the way in which ω_0 was fixed. If one instead sets its value by matching the bulk speed of sound in KBr, the time unit increases by a factor 1.7, with a corresponding decrease in the energy scale.

For the various nonlinearity parameters, λ, etc., we took values in the same range that other authors have used [16]. The push from the expanded quasimolecule is expressed through the nondynamic q_0 which was taken to be 1. With this value the equilibrium position of the Br is displaced by about 8% of the ion separation distance and the instantaneous push somewhat more.

The "holding" parameter ν was taken to be 4, reflecting the number of off-chain nearest neighbors each ion has.

For the runs reported in this article we used 40 ions, although in many previous numerical integrations other numbers were used, with little change unless there were fewer than 10. Similar remarks apply to most of the other parameters.

[1] R. Reigada, A. Sarmiento, and K. Lindenberg, Phys. Rev. E **64**, 066608 (2001).

[2] S. Flach and C. Willis, Phys. Rep. **295**, 181 (1998).

[3] U. T. Schwarz, L. Q. English, and A. J. Sievers, Phys. Rev. Lett. **83**, 223 (1999).

[4] K. Polák, M. Nikl, and E. Mihóková, J. Lumin. **54**, 189 (1992).

[5] J. Hlinka, E. Mihóková, and M. Nikl, Phys. Status Solidi B **166**, 503 (1991).

[6] J. Hlinka, E. Mihóková, M. Nikl, K. Polák, and J. Rosa, Phys. Status Solidi B **175**, 523 (1993).

[7] E. Mihóková, M. Nikl, K. Polák, and K. Nitsch, J. Phys.: Condens. Matter **6**, 293 (1994).

[8] M. Nikl, J. Hlinka, E. Mihóková, K. Polák, P. Fabeni, and G. P. Pazzi, Philos. Mag. B **67**, 627 (1993).

[9] B. Gaveau, E. Mihóková, M. Nikl, K. Polák, and L. S. Schulman, Phys. Rev. B **58**, 6938 (1998).

[10] B. Gaveau, E. Mihóková, M. Nikl, K. Polák, and L. S. Schul-

man, J. Lumin. **92**, 311 (2001).
[11] E. Mihóková, L. S. Schulman, M. Nikl, B. Gaveau, K. Polák, K. Nitsch, and D. Zimmerman, Phys. Rev. B **66**, 155102 (2002).
[12] L. S. Schulman, E. Mihóková, A. Scardicchio, P. Facchi, M. Nikl, K. Polak, and B. Gaveau, Phys. Rev. Lett. **88**, 224101 (2002).
[13] L. S. Schulman, Phys. Rev. A **68**, 052109 (2003).
[14] E. Fermi, J. Pasta, and S. Ulam, Technical Report, Los Alamos (1955), reprinted in *Enrico Fermi, Collected Papers, Volume II* (University of Chicago Press, Chicago, 1965), article 266, p. 978.
[15] A. J. Lichtenberg and M. A. Lieberman, *Regular and Stochastic Motion* (Springer, New York, 1983).
[16] S. R. Bickham and A. J. Sievers, Phys. Rev. B **43**, 2339 (1991).
[17] S. R. Bickham, S. A. Kiselev, and A. J. Sievers, Phys. Rev. B **47**, 14 206 (1993).
[18] V. M. Burlakov, S. A. Kiselev, and V. N. Pyrkov, Phys. Rev. B **42**, 4921 (1990).
[19] O. A. Chubykalo, A. S. Kovalev, and O. V. Usatenko, Phys. Lett. A **178**, 129 (1993).
[20] R. Dusi and M. Wagner, Phys. Rev. B **51**, 15 847 (1995).
[21] R. Dusi, G. Viliani, and M. Wagner, Phys. Rev. B **54**, 9809 (1996).
[22] V. Fleurov, R. Schilling, and S. Flach, Phys. Rev. E **58**, 339 (1998).
[23] S. A. Kiselev, S. R. Bickham, and A. J. Sievers, Phys. Rev. B **50**, 9135 (1994).
[24] J. B. Page, Phys. Rev. B **41**, 7835 (1990).
[25] A. J. Sievers and S. Takeno, Phys. Rev. Lett. **61**, 970 (1988).
[26] B. I. Swanson, J. A. Brozik, S. P. Love, G. F. Strouse, A. P. Shreve, A. R. Bishop, W.-Z. Wang, and M. I. Salkola, Phys. Rev. Lett. **82**, 3288 (1999).
[27] S. Takeno and A. J. Sievers, Solid State Commun. **67**, 1023 (1988).
[28] Y. Zolotaryuk, S. Flach, and V. Fleurov, Phys. Rev. B **63**, 214422 (2001).
[29] Since the publication of Ref. [9], Ranfagni *et al.* [43] have proposed an alternative explanation of the anomaly based on tunneling between emission bands. For Th this effect may contribute, but for Pb (as the impurity), for which the anomaly is especially strong, no second emission band has been observed.
[30] A. Ranfagni, D. Mugnai, M. Bacci, G. Villiani, and M. P. Fontana, Adv. Phys. **32**, 823 (1983).
[31] P. W. M. Jacobs, J. Phys. Chem. Solids **52**, 35 (1991).
[32] The $PbBr_6$ quasimolecule can also *shrink* along the JT axis, in which case all instances of the word "push" in this article should be changed to "pull." For our simulations this makes no difference. We found confinement with $q_0<0$ as well as $q_0>0$.
[33] J. Andriessen, M. Marsman, and C. W. E. van Eijk, J. Phys.: Condens. Matter **13**, 10 507 (2001).
[34] Ref. [23] discusses "intrinsic" localized modes, working in a translationally invariant context, which is not the case in our situation.
[35] K. Takatsuka, J. Comput. Phys. **102**, 374 (1992).
[36] In principle, the loop we see could be the projection from a higher dimensional structure. This would be a (nongeneric) coincidence, but coincidences do happen. Nevertheless, that is not occurring here. In our investigations we simultaneously viewed more than one projection of the torus, and when there was a one-dimensional loop in one plane, there was a one-dimensional loop in the others. This can be seen in Fig. 4(d), where we actually do show more than one plane.
[37] K. Polák (private communication).
[38] A. Soffer (private communication).
[39] The various symmetries mentioned, A_{1u}, A_{1g}, and T_{1g}, refer to representations of the O_h group.
[40] G. Boulon, in *Spectroscopy of Solid State Laser-Type Materials*, edited by B. DiBartolo (Plenum Press, New York, 1987), p. 223.
[41] A. E. Hughes and G. P. Pells, Phys. Status Solidi B **71**, 707 (1975).
[42] S. Flach, C. R. Willis, and E. Olbrich, Phys. Rev. E **49**, 836 (1994).
[43] A. Ranfagni, D. Mugnai, P. Fabeni, and G. P. Pazzi, Phys. Rev. B **66**, 184107 (2002).